Intracellular Dual Fluorescent Lightup Bioprobes for Image-Guided Photodynamic Cancer Therapy

Haijie Han, Qiao Jin, Haibo Wang, Wenzhuo Teng, Jina Wu, Hongxin Tong, Tingting Chen, and Jian Ji**

An intracellular dual fluorescent light-up bioprobe with aggregation-induced emission features and endogenously producing photosensitizer protoporphyrin IX (PpIX) abilities is designed and synthesized. The bioprobe is nonemissive in physiological environment. However, the bioprobe can selectively light up cancer cells with blue fluorescence of tetraphenylene (TPE) and red fluorescence of PpIX, owing to the release of TPE and methyl aminolevulinate after targeted internalization by cancer cells. Moreover, upon endogenous generation and accumulation of PpIX in cancer cells, efficient photodynamic ablation of cancer cells after light irradiation is demonstrated with easy regulation for optimal therapeutic efficacy. The design of such dual fluorescent light-up bioprobes might provide a new opportunity for targeted and image-guided photodynamic cancer therapy.

1. Introduction

Image-guided delivery systems that combine diagnostic agents and therapeutic drugs in a single formulation have attracted much attention for precision medicine.[1–4] The fluorescent probe can not only be considered as one of the most effective diagnostic tools for real-time and noninvasive monitor of biological processes, but it also serves as a powerful tool for the development of personalized medicine and targeted therapies.[5] However, the conventional fluorophore always suffers from low sensitivity and signal-to-noise ratio owing to the intrinsically fluorescence with high background signals. In order to tackle this challenge, it is urgently needed if the fluorophore is in "OFF" stage and the fluorescence can be activated only in a specific environment. Recently, to reduce false-positive responses, the fluorescent lightup bioprobes that can respond to specific signals are developed for diagnosis and tracking of many diseases because of the high sensitivity and low background signals.[6] In addition, the conventional fluorophore can usually result in aggregation-caused quenching effect. Fluorogens with aggregation-induced emission (AIE) behaviors have recently been developed as a powerful tool for bioimaging.[7–10] Unlike the conventional fluorescent dyes, AIE bioprobes show weak or no fluorescence in molecularly dissolved state. However, strong fluorescence can be observed when they are in aggregated state because of the restriction of intramolecular free rotations. Based on the unique AIE characteristics, the AIE molecules are especially attractive to construct fluorescent lightup bioprobes in response to biological stimuli, such as pH, redox potential, and dysregulated enzymes.[11–17] Unfortunately, only single fluorescent lightup bioprobes were reported so far. It will be particularly interesting to design dual fluorescent lightup bioprobes, which might show higher sensitivity and signal-to-noise ratio.

Photodynamic therapy (PDT), which is both minimally invasive and minimally toxic, is considered as a favorable

H. Han, Dr. Q. Jin, W. Teng, J. Wu, H. Tong, T. Chen, Prof. J. Ji
MOE Key Laboratory of Macromolecular Synthesis and Functionalization
Department of Polymer Science and Engineering
Zhejiang University
Hangzhou 310027, China
E-mail: jinqiao@zju.edu.cn; jijian@zju.edu.cn
Dr. H. Wang
Textile Institute
College of Light Industry
Textile and Food Engineering
Sichuan University
Chengdu 610065, China

DOI: 10.1002/smll.201600950

www.MaterialsViews.com

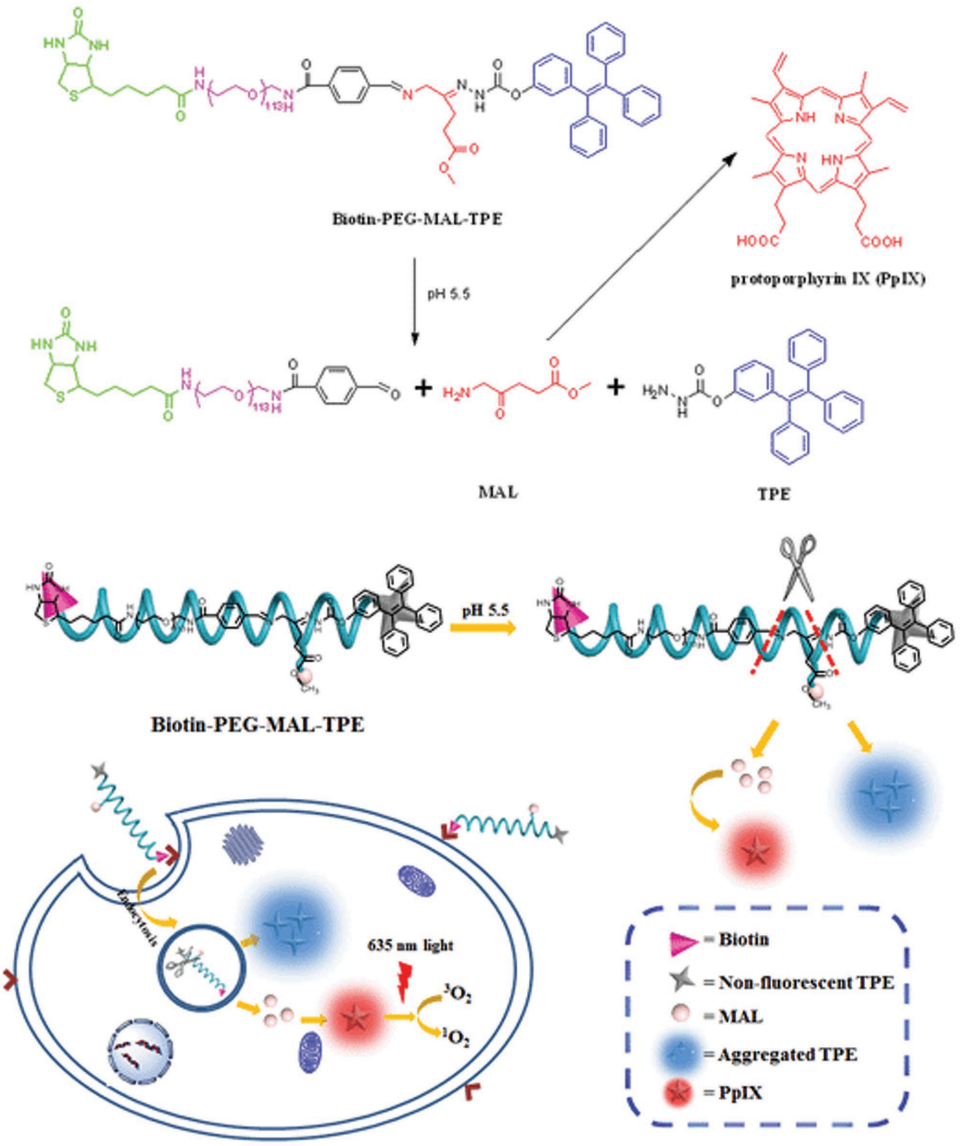

Figure 1. Schematic illustration of the intracellular dual fluorescent lightup of Biotin-PEG-MAL-TPE.

modality for the treatment of tumor and other different diseases.[18–22] However, the choice of clinically used PDT drugs is extremely limited since only Photofrin, Visudyne, and Levulan (5-aminolevulinic acid, ALA) are approved by U.S. FDA.[23] Compared to exogenously administered photosensitizers, ALA which can be metabolized to the photosensitizer protoporphyrin IX (PpIX) via intracellular heme biosynthetic pathway is gaining increasing attention because of its fast clearance and reduced concomitant photosensitivity.[24] ALA and its derivatives such as methyl aminolevulinate (MAL) have been successfully used for the treatment of different malignancies, such as actinic keratosis, basal cell carcinoma, bladder cancer, etc.[25–29] Meanwhile, taking advantage of ALA-induced PpIX fluorescence, ALA and its derivatives have great potential as a diagnostic agent for cancer diagnosis and fluorescence-guided surgery for resection of malignant tumors.[30] However, because of the hydrophilic nature and low specificity to tumor cells, the cellular internalization of ALA and its derivatives is greatly limited by the lipophilic membrane barrier.[31,32] It would be highly desirable to develop new delivery systems to bypass the lipophilic barrier so that ALA and its derivatives can be effectively internalized by cancer cells. Nevertheless, efficient delivery vehicles for targeted delivery of ALA and its derivatives are still largely unexplored up to now.

In this research, we designed a proof-of-concept bioprobe based on ALA prodrug and AIE fluorogen that can be utilized for endogenous dual fluorescent lightup bioimaging and targeted photodynamic cancer therapy (**Figure 1**). Such theranostic prodrug Biotin-PEG-MAL-TPE contains: (1) a photosensitizer precursor MAL, which can be converted to the photosensitizer PpIX for PDT and fluorescent lightup imaging; (2) a tetraphenylene (TPE) unit with typical AIE properties for fluorescent lightup imaging; (3) a PEG polymer chain to increase the hydrophilicity, and (4) a biotin molecule as a targeting moiety. MAL and TPE were conjugated to the back bone via pH responsive covalent bonds. Meanwhile, the prodrug Biotin-PEG-TPE in which TPE was conjugated

small 2016,
DOI: 10.1002/smll.201600950

to PEG via stable amide bond was used as a control to investigate pH-responsive fluorescent lightup. The prodrug PEG-MAL-TPE without biotin targeting was also used as a control to study the targeting ability of biotin. Biotin-PEG-MAL-TPE prodrug is water soluble and expected to be non-fluorescent in physiological environment. After cell uptake, the acid-labile hydrazone bond and benzoic imine bond could be cleaved, which could result in the release of MAL and TPE.[33,34] Therefore, such prodrug offers a good opportunity to develop activatable photosensitizer with dual fluorescent lightup properties for image-guided photodynamic ablation of cancer cells.

2. Results and Discussion

The prodrug Biotin-PEG-MAL-TPE was synthesized through a multiple synthesis process as shown in Scheme S4 (Supporting Information). MAL and TPE were conjugated to PEG back bone via acid-labile benzoic imine bond and hydrazone bond. Meanwhile, the bioprobe Biotin-PEG-TPE without pH responsiveness and PEG-MAL-TPE without biotin targeting were synthesized as negative controls (Schemes S5 and S6, Supporting Information). The successful synthesis of Biotin-PEG-MAL-TPE, Biotin-PEG-TPE, and PEG-MAL-TPE was confirmed by ^{1}H NMR, ^{13}C NMR, ESI-MS, and FT-IR (Figures S1–S22, Supporting Information).

It is well known that TPE shows typical AIE characteristics. The fluorescent emission spectra of Biotin-PEG-MAL-TPE probe and hydrazide functionalized TPE (TPE-hyd) in DMSO/PBS mixture (1/99, v/v) were shown in **Figure 2**. The hydrophobic TPE-hyd showed strong blue fluorescence, whereas Biotin-PEG-MAL-TPE probe was almost nonfluorescent in the same medium owing to the excellent hydrophilicity. Such probe was also stable and remained non-fluorescent in cell culture medium or phosphate-buffered saline (PBS) (Figure S23, Supporting Information). Therefore, Biotin-PEG-MAL-TPE is very promising to serve as a lightup probe with minimal background signals.

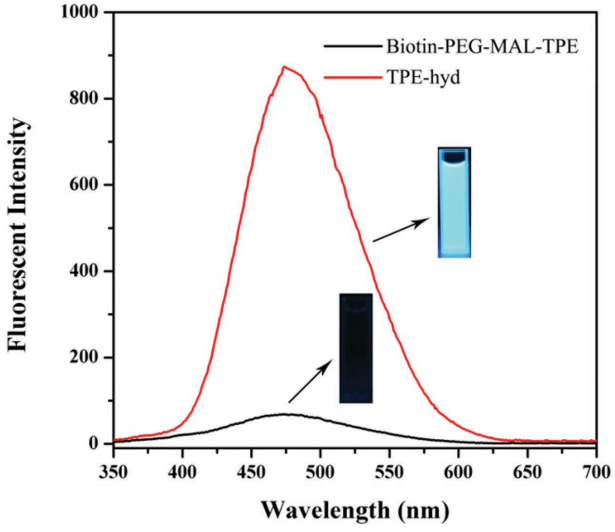

Figure 2. Fluorescent emission spectra of 50×10^{-6} M Biotin-PEG-MAL-TPE bioprobe and 50×10^{-6} M TPE-hyd with excitation of 360 nm in DMSO/PBS mixture (1/99, v/v, pH 7.4). Inset: Corresponding digital photographs taken under 365 nm irradiation.

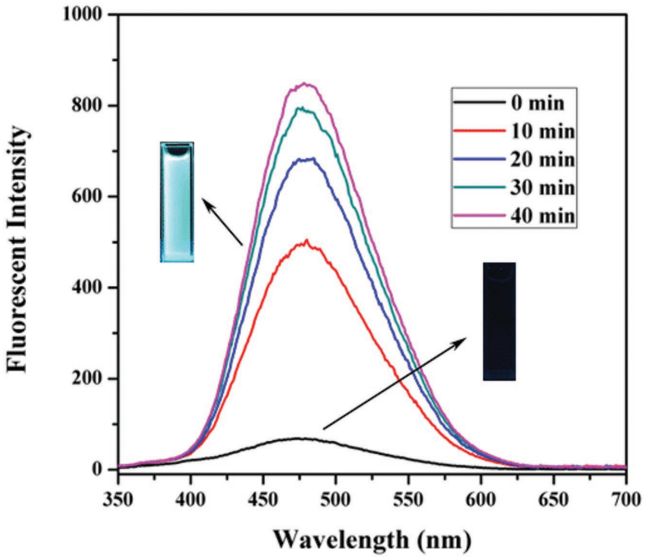

Figure 3. Time-dependent fluorescent emission spectra of 50×10^{-6} M Biotin-PEG-MAL-TPE bioprobe with excitation of 360 nm at pH 5.5. Inset: Corresponding digital photographs taken under 365 nm irradiation.

The response of Biotin-PEG-MAL-TPE to different pH was evaluated by incubation of the probe at pH 7.4, 6.8, and 5.5. The fluorescent emission spectra were recorded over time. As shown in Figure S24 (Supporting Information), the Biotin-PEG-MAL-TPE probe was almost nonemissive and negligible fluorescence change was observed over time at pH 7.4. Interestingly, the fluorescent emission intensity of Biotin-PEG-MAL-TPE increased significantly with time at pH 5.5 (**Figure 3**). Strong blue fluorescence of TPE was observed after incubation at pH 5.5 for 40 min owing to the cleavage of acid-labile chemical bonds. The hydrophobic TPE-hyd was released from hydrophilic Biotin-PEG-MAL-TPE and preferred to be aggregated in PBS solution. In order to obtain the direct evidence of the cleavage of acid-labile chemical bonds as well as pH-responsive release of photosensitizer precursor MAL, ^{1}H NMR was used to study the structural change of Biotin-PEG-MAL-TPE in acidic environment (**Figure 4**). After incubation in acidic environment for 24 h, the peak at 1.9 ppm assigned to —CH_2— next to hydrazone bond disappeared. Meanwhile, a new peak at 2.9 ppm assigned to —CH_2— next to keto group appeared, which showed the cleavage of hydrazone bond. The cleavage of benzoic imine bond was confirmed by the disappearance of the peak at 8.6 ppm arising from —CH = N— together with the appearance of the peak at 10.1 ppm of —CHO. Therefore, the benzoic imine bond and hydrazone bond can be cleaved in acidic environment, accompanied with the release of MAL and TPE residue. Furthermore, the molecular dissolution of the prodrug and the aggregation of the cleaved TPE residues were further confirmed by dynamic light scattering (DLS). Biotin-PEG-MAL-TPE was molecularly dissolved in PBS with hydrodynamic diameter of 2.3 nm. However, after incubation at pH 5.5 for 30 min, the hydrophobic TPE

DOI: 10.1002/smll.201600950

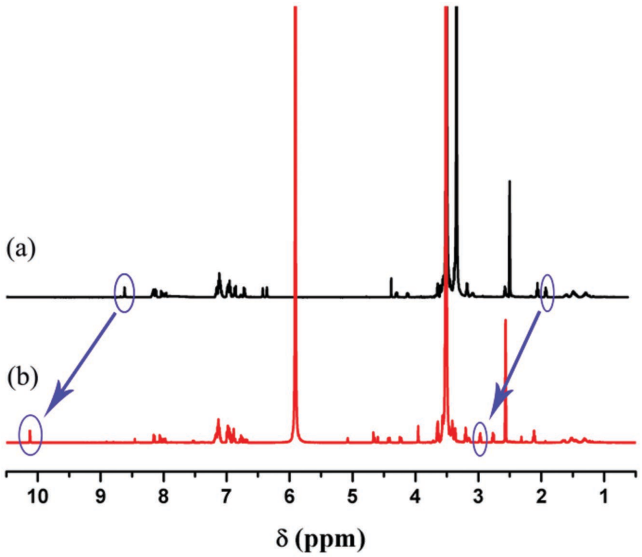

Figure 4. ^{1}H NMR spectra of Biotin-PEG-MAL-TPE in a) DMSO-d_6 and b) DMSO-d_6 with 2% deuterium chloride for 24 h (pH 3.1).

residues tended to cluster into aggregates as confirmed by DLS (Figure S25, Supporting Information). The aggregation of TPE residues can restrict the intramolecular rotations and pH-responsive fluorescent lightup was realized.

Intracellular lightup imaging was studied using A549 (human lung adenocarcinoma epithelial cell line) as a model cancer cell line. HUVEC (human umbilical vein endothelial cell line) was used as a control normal cell line with less receptor of biotin. As discussed above, the Biotin-PEG-MAL-TPE probe was nonemissive before cell uptake. Surprisingly, after incubation of Biotin-PEG-MAL-TPE probes with A549 cancer cells for 8 h, strong intracellular blue fluorescence and red fluorescence were observed (**Figure 5**a). Such intracellular dual fluorescent lightup was most probably because of the pH-responsive release of TPE and MAL. The cellular internalization mechanism and pathway for Biotin-PEG-MAL-TPE bioprobes were further investigated. Since endocytosis is an energy-dependent uptake process for various extracelluar substances and can usually be inhibited by incubating cells at low temperature (4 °C instead of 37 °C) or in ATP (adenosine triphosphate) depleted environments such as pretreating with NaN_3.[35,36] Cell culture was carried out at 4 °C or pretreated with NaN_3 in parallel with regular incubation conditions to investigate the cellular internalization pathway. Indeed, the fluorescence of the cells incubated at 4 °C or pretreated with NaN_3 was much weaker, which further confirmed that Biotin-PEG-MAL-TPE was internalized into cells by endocytosis (Figure S27, Supporting Information). After biotin-mediated selective endocytosis, Biotin-PEG-MAL-TPE probe was internalized into the lysosome. The hydrazone bond and benzoic imine bond were unstable in acidic lysosomal environment. Therefore, TPE and MAL can be released. After TPE was cleaved, strong blue fluorescence lightup was observed because of the AIE effect. Meanwhile, after MAL was released, MAL can be converted into the photosensitizer PpIX by intracellular heme biosynthetic pathway. Strong red fluorescence lightup of PpIX can hence be observed. Moreover, it is well known

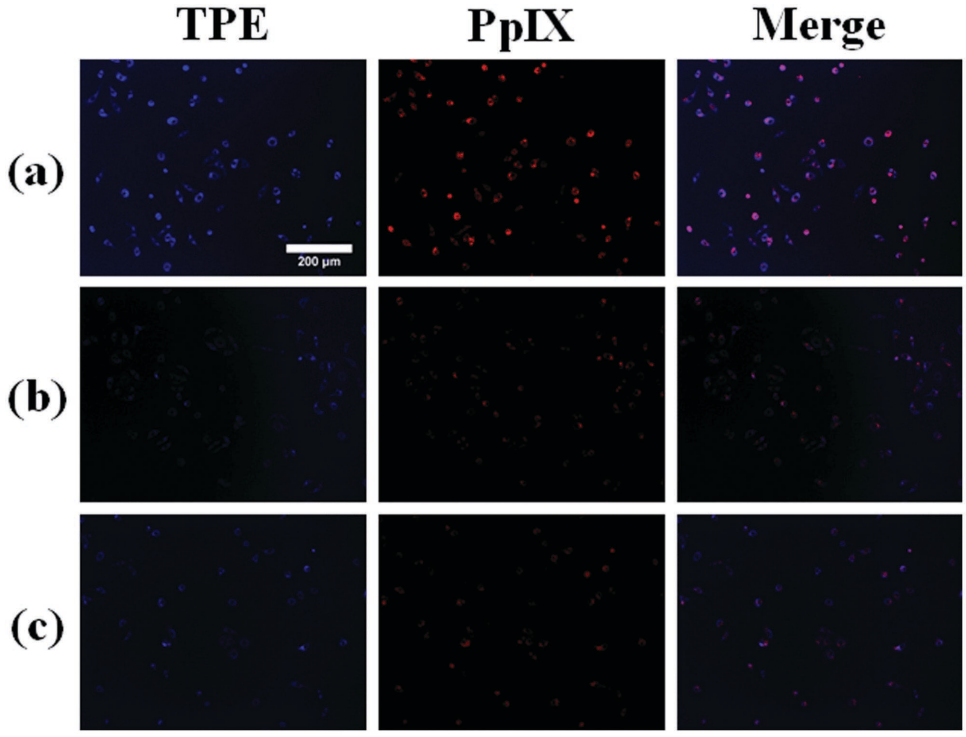

Figure 5. Fluorescence microscopy images of a) A549 cells incubated with 50×10^{-6} M Biotin-PEG-MAL-TPE bioprobes for 8 h, strong intracellular blue fluorescence of TPE, and red fluorescence of PpIX were observed; b) HUVEC cells incubated with 50×10^{-6} M Biotin-PEG-MAL-TPE bioprobes for 8 h, weak fluorescence was observed owing to the less receptor of biotin in HUVEC cells; c) A549 cells incubated with 50×10^{-6} M PEG-MAL-TPE bioprobes for 8 h, very weak fluorescence was observed owing to the absence of biotin moieties.

DOI: 10.1002/smll.201600950

small NANO MICRO

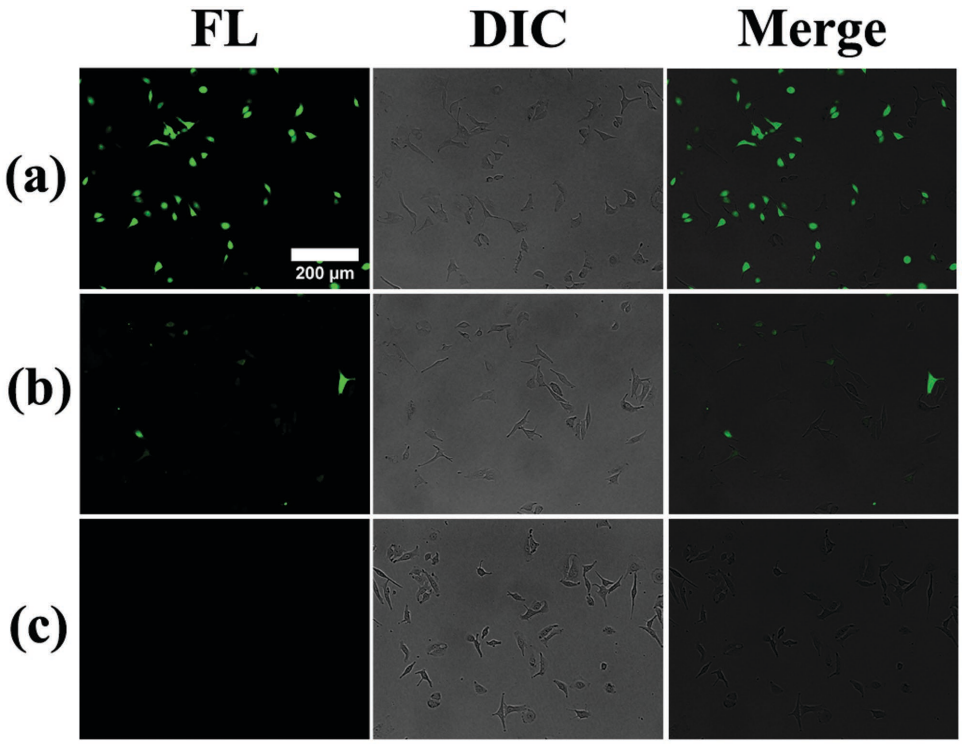

Figure 6. Reactive oxygen generation detected by fluorescence of DCFDA in A549 cells exposed to a) Biotin-PEG-MAL-TPE prodrug after irradiated with 635 nm light at 500 mW cm^{-2} for 0.5 min. b) PEG-MAL-TPE prodrug, after irradiated with 635 nm light at 500 mW cm^{-2} for 0.5 min and c) control without treatment.

that biotin can increase the selective uptake by cancer cells via receptor-mediated endocytosis.[37,38] If Biotin-PEG-MAL-TPE probes were incubated with HUVEC cells for 8 h, only weak fluorescence of TPE and PpIX could be observed in HUVEC cells, which might be ascribed to the less receptor of biotin in HUVEC cells (Figure 5b). Therefore, Biotin-PEG-MAL-TPE bioprobes can selectively light up cancer cells in a high signal-to-noise ratio. At the same time, PEG-MAL-TPE prodrugs without biotin targeting were also used as negative control. As shown in Figure 5c, after incubation of PEG-MAL-TPE with A549 cells, the fluorescent intensity of A549 cells was much weaker than that incubated with Biotin-PEG-MAL-TPE, probably owing to the inefficient cellular internalization. Meanwhile, if A549 cells were incubated with Biotin-PEG-TPE, in which TPE was conjugated to PEG by stable amide bonds, blue fluorescence was not able to be observed in A549 cells since TPE cannot be cleaved from the probe in lysosomal pH (Figure S28, Supporting Information). Therefore, by unique molecular design of Biotin-PEG-MAL-TPE, intracellular dual fluorescence lightup can be detected in cancer cells, which might be very promising for bioimaging.

The generation of reactive oxygen species (ROS) upon light irradiation of a photosensitizer plays an important role for the apoptosis of cancer cells in PDT. MAL is a precursor of the strong photosensitizer PpIX. PpIX can generate ROS upon red light irradiation, which is highly cytotoxic and can lead to cell apoptosis. As shown in Figure 5, strong red fluorescence of PpIX can be observed after incubation of the prodrugs with A549 cells, which indicated successful generation and accumulation of PpIX in cancer cells. The ROS generated by endogenous PpIX after 635 nm red light irradiation was further studied by staining A549 cells with 2′,7′-dichlorofluorescein diacetate (DCFDA).[39] DCFDA is nonfluorescent and can be oxidized to 2′,7′-dichlorofluorescein (DCF) by ROS, which shows strong green fluorescence. The green fluorescence was imaged by fluorescence microscopy. As expected, because of the selective internalization of Biotin-PEG-MAL-TPE prodrug by receptor-mediated endocytosis, the green fluorescence of A549 cells incubated with Biotin-PEG-MAL-TPE prodrug was much stronger than that of PEG-MAL-TPE prodrug (**Figure 6**), which was consistent with the accumulation of PpIX in A549 cells (Figure 5a).

Since the production of ROS is a major mediator for the activation of apoptosis signaling pathways in PDT, the influence of Biotin-PEG-MAL-TPE and PEG-MAL-TPE prodrugs on cancer cell apoptosis after light irradiation was evaluated by the annexin V conjugate staining assay. The flow cytometry results are shown in **Figure 7** and the sum of the two right quadrants represents apoptosis. After A549 cells were incubated with Biotin-PEG-MAL-TPE prodrugs and irradiated with 635 nm laser for 1 min, 36% of cancer cells were induced to undergo apoptosis. However, the apoptosis of A549 cells incubated with PEG-MAL-TPE prodrugs was only 22%. Therefore, Biotin-PEG-MAL-TPE prodrugs can cause cell apoptosis to a greater extent than PEG-MAL-TPE prodrugs, which was in good agreement with the generation of PpIX and ROS.

It is very important for a practical system of PDT that it exhibits low cytotoxicity without light irradiation and can induce high cytotoxicity after light irradiation. The

DOI: 10.1002/smll.201600950

www.MaterialsViews.com

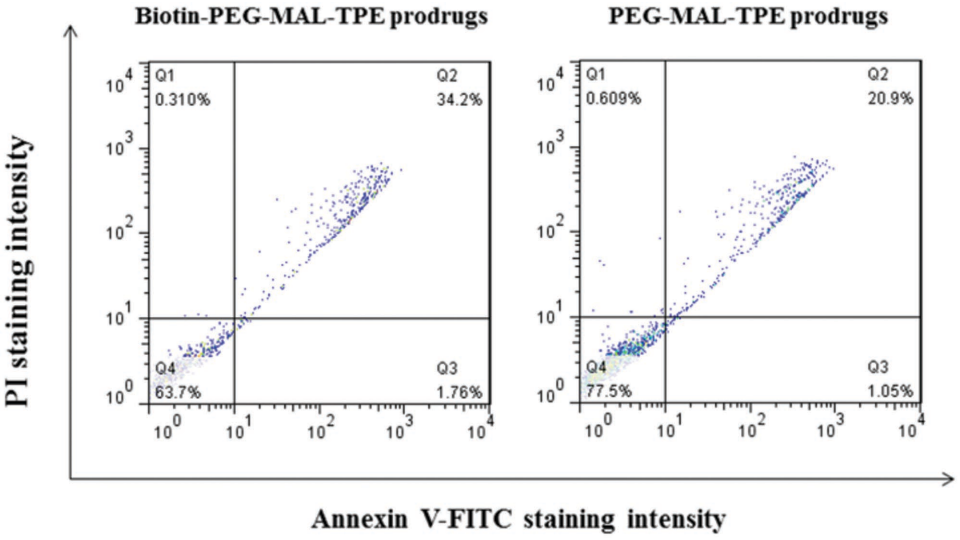

Figure 7. Induction of apoptosis on A549 cells after incubation with Biotin-PEG-MAL-TPE prodrugs and PEG-MAL-TPE prodrugs.

photodynamic cytotoxicity of the prodrugs was evaluated by MTT assay with light irradiation at 635 nm. At first, the dark cytotoxicity of Biotin-PEG-MAL-TPE prodrugs, PEG-MAL-TPE prodrugs, and free MAL against A549 cells was evaluated. As shown in **Figure 8**a, after 24 h incubation, all the samples did not show obvious cytotoxicity without light irradiation even when the concentration of MAL was as high as 50×10^{-6} M. However, a dose-dependent cytotoxicity was observed in A549 cells upon exposure to 635 nm light for 5 min (Figure 8b). Compared to PEG-MAL-TPE prodrugs and free MAL, Biotin-PEG-MAL-TPE prodrugs exhibited a higher percentage of cell death with half-maximal inhibitory concentration (IC_{50}) of 12.3×10^{-6} M. The results were consistent with the ROS generation as well as the apoptosis studies. Meanwhile, the photodynamic cytotoxicity can be well regulated by irradiation time and light intensity. As expected, stronger inhibition of cell viability was observed with longer irradiation time or stronger light intensity

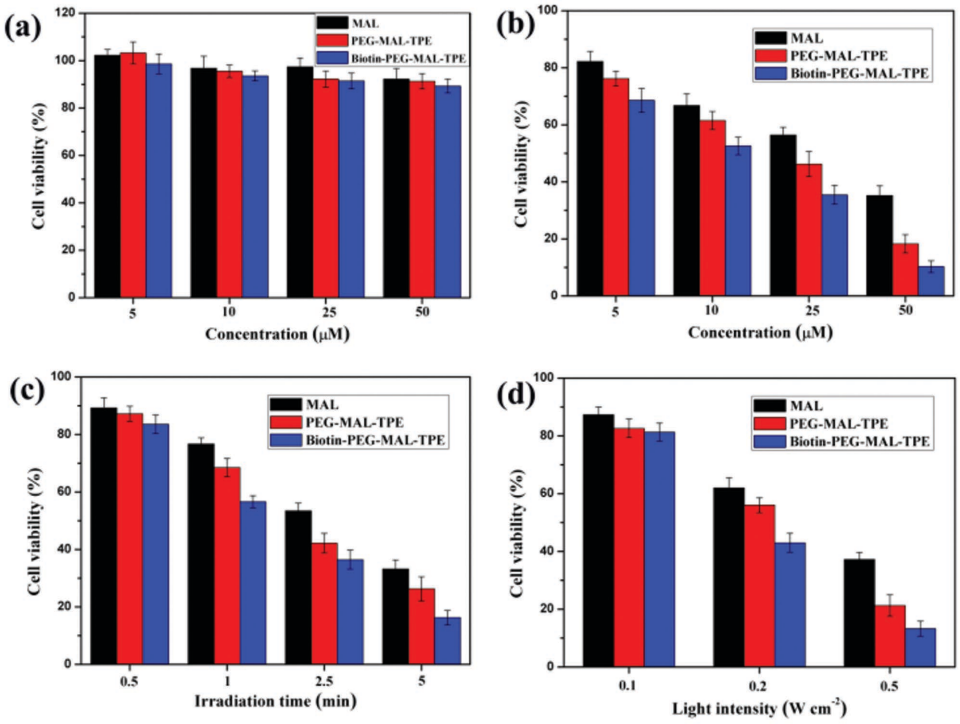

Figure 8. Cell viability of A549 cells a) after incubation with the prodrugs at different concentrations without light irradiation for 24 h; b) upon incubation with the prodrugs at different concentrations after 5 min light irradiation (500 mW cm^{-2}) followed by further incubation for 24 h; c) upon incubation of the cells with 50×10^{-6} M prodrugs and irradiation with light (500 mW cm^{-2}) for different time, followed by further incubation for 24 h; d) upon incubation of the cells with 50×10^{-6} M prodrugs and irradiation with different light intensity for 5 min, followed by further incubation for 24 h.

small 2016,
DOI: 10.1002/smll.201600950

(Figure 8c,d). Therefore, the photodynamic cytotoxicity of the prodrugs could be easily regulated for optimal results and hence can be considered as ideal vehicles for PDT.

3. Conclusion

In summary, a pH-responsive bioprobe Biotin-PEG-MAL-TPE was successfully synthesized and utilized for intracellular dual fluorescent lightup imaging and targeted photodynamic ablation of cancer cells. Biotin-PEG-MAL-TPE bioprobe was almost nonfluorescent in physiological environment. After internalized into A549 cancer cells, TPE and MAL can be released in acidic lysosomal environment. Intracellular dual fluorescent lightup was achieved owing to the AIE effect of TPE and heme biosynthesis of PpIX from MAL. Importantly, benefiting from the biotin targeting ligand, such Biotin-PEG-MAL-TPE bioprobe, can selectively light up cancer cells with both blue fluorescence of TPE and red fluorescence of PpIX. The endogenously generated PpIX was further used as a photosensitizer for PDT. After 635 nm light irradiation, Biotin-PEG-MAL-TPE prodrugs exhibited stronger inhibition of cell viability than PEG-MAL-TPE prodrugs and free MAL. In order to achieve optimal PDT, the photodynamic cytotoxicity of the prodrugs could be easily regulated by changing the concentration of MAL, irradiation time, as well as light intensity. The design of endogenous dual fluorescent lightup bioprobes presents a promising potential for targeted image-guided photodynamic cancer therapy.

4. Experimental Section

Materials: N-(3-dimethylaminopropyl)-*N*′-ethylcarbodiimide HCl (EDC), *N*-hydroxysuccinimide (NHS), dicyclohexylcarbodiimide (DCC), 4-dimethylaminopyridine (DMAP), and ethyl bromoacetate were purchased from Sigma-Aldrich. 3-(4,5-dimethyl-thiazol-2-yl)-2,5-diphenyl tetrazolium bromide (MTT) was purchased from YEASEN. Benzophenone, 4-hydrobenzopheone, 4-formyl benzoic acid, and hydrazine hydrate were purchased from Energy Chemical. Zinc powder and titanium tetrachloride ($TiCl_4$) were obtained from Sinopharm Chemical Reagent Co., Ltd. Biotin-PEG5000-NH_2 and mPEG5000-NH_2 were purchased from Xi'an ruixi Biological Technology Co., Ltd. Methyl 5-aminolevulinate hydrochloride (MAL·HCl) was obtained from J&K Scientific Ltd. A549 cell line and HUVEC cell line were obtained from KeyGEN BioTECH.

Characterization: ^{1}H NMR spectra and ^{13}C NMR spectra were recorded on a Bruker DMX500 instrument. Mass spectra were recorded on Bruker Esquire 3000 plus. Fourier transform infrared spectroscopy (FT-IR) analyses were performed on a Bruker Vector2 spectrometer. Fluorescence emission spectra were recorded from PerkinElmer LS 55 fluorescence spectrometer. DLS measurements were performed using Zetasizer Nano-ZS from Malvern Instruments equipped with a He-Ne laser at wavelength of 633 nm at 25 °C. Intensity-average hydrodynamic diameter (Dh) was adopted in this research. Transmission electron microscopy (TEM) was performed on a JEM-1230EX TEM (JEOL, Japan) operated at the accelerating voltage of 80 kV.

Synthesis of TPE-hyd: TPE-hyd was prepared according to our previous publication.[40] Under an Ar atmosphere, benzophenone (36.4 g, 0.2 mol), 4-hydrobenzopheone (38 g, 0.2 mol), zinc powder (32 g, 0.48 mol), and 600 mL of THF were added into a three-necked flask under stirring at 0 °C. 26 mL of $TiCl_4$ (0.24 mol) was then slowly added. The mixture was stirred at room temperature for 0.5 h and then refluxed overnight. After cooled to room temperature, 100 mL of 1 M dilute hydrochloric acid was added and extracted with dichloromethane (CH_2Cl_2). The crude product was purified by a silica gel column (petroleum ether:ethyl acetate = 15:1). Hydroxylated TPE (TPE-OH) was obtained as a white solid. 3.34 g of ethyl bromoacetate (20 mmol), 7 g of TPE-OH (20 mmol), 4 g of K_2CO_3 (30 mmol), and 100 mL of acetonitrile were added into a flask. The mixture was refluxed over night at 100 °C. The resulting mixture solution was separated by filtration. The crude TPE-Et was purified through silica gel column (petroleum ether:ethyl acetate = 20:1). Finally, 1 g of TPE-Et was dissolved into methanol. Then, hydrazine hydrate (3 mL) was added and stirred vigorously. After 10 h, the mixture solution was poured into water and extracted with CH_2Cl_2 for three times. The collected organic layer was concentrated under reduced pressure. ^{1}H NMR (500 MHz, DMSO-d6) δ 4.31 (s, 2H), 4.39 (s, 2H), 6.73 (d, 2H), 6.86 (d,2H), 6.97 (q, 6H), 7.11 (m, 9H), 9.30 (s, 1H). ^{13}C NMR (125 MHz, DMSO-d6) δ 66.15, 113.95, 126.47, 127.80, 130.64, 131.78, 136.15, 139.94, 143.54, 156.25, 166.69. MS (EI): M+m/z 421.3.

Synthesis of Succinimidyl 4-Formylbenzoate: Succinimidyl 4-formylbenzoate was synthesized as previously described.[41] 2 g of 4-formyl benzoic acid (13.3 mmol) was dissolved in 50 mL of acetonitrile. 2.8 g of *N*-(3-dimethylaminopropyl)-*N*′-ethylcarbodiimide HCl (EDC, 14.6 mmol) and 1.7 g of NHS (14.6 mmol) were then added. The solution was stirred overnight at room temperature. Acetonitrile was removed in vacuum and replaced by CH_2Cl_2 and washed three times with water. The solution was dried over $MgSO_4$ and CH_2Cl_2 was removed in vacuum. Succinimidyl 4-formylbenzoate was obtained as white powder. ^{1}H NMR (500 MHz, $CDCl_3$) δ 2.94 (s, 4H), 8.03 (d, 2H), 8.30 (d, 2H), 10.14 (s,1H). ^{13}C NMR (125 MHz, $CDCl_3$) δ 25.84, 129.76, 131.11, 140.57, 161.08, 169.16, 191.30.

Synthesis of Carboxylated TPE: Carboxylated TPE (TPE-COOH) was prepared according to our previous publication with slight modification.[42] Benzophenone (36.4 g, 0.2 mol), 4-hydrobenzopheone (38 g, 0.2 mol), zinc powder (32 g, 0.48 mol), and 600 mL of THF were added into a three-necked flask under stirring at 0 °C. 26 mL of $TiCl_4$ (0.24 mol) was then slowly added. The mixture was stirred at room temperature for 0.5 h and then refluxed overnight. After cooled to room temperature, 100 mL of dilute hydrochloric acid (1 mol L^{-1}) was added and extracted with CH_2Cl_2. The crude product was purified by a silica gel column and TPE-OH was obtained as a white solid. 3.34 g of ethyl bromoacetate (20 mmol), 7 g of TPE-OH (20 mmol), 4 g of K_2CO_3 (30 mmol), and 100 mL of acetonitrile were added into a flask. The mixture was refluxed over night at 100 °C. The resulting mixture solution was separated by filtration. The crude was purified through silica gel column. This product was added into a solution (CH_2Cl_2:TFA = 1:1) and stirred vigorously. After 24 h, the mixture solution was poured into water and extracted with CH_2Cl_2 for three times. The collected organic layer was concentrated under reduced pressure. TPE-COOH was obtained as white powder. ^{1}H NMR (500 MHz, $CDCl_3$) δ 4.60 (s, 2H), 6.65 (d, 2H), 6.95 (d,2H), 7.02 (q, 6H), 7.09 (m, 9H). ^{13}C NMR (125 MHz, $CDCl_3$) δ 59.52,

DOI: 10.1002/smll.201600950

108.58, 121.23, 126.07, 127.47, 132.43, 134.87, 135.41, 138.56, 150.59, 168.67. MS (EI): M-m/z 405.4.

Synthesis of MAL Conjugated TPE: MAL was conjugated to TPE-hyd via acid-labile benzoic imine bond. Briefly, 200 mg of TPE-hyd (0.37 mmol) and 127 mg of MAL (0.7 mmol) were dissolved in 10 mL of DMSO. A drop of trifluoroacetic acid was then added. The resulting solution was stirred at room temperature. After 24 h, the crude product was purified by a silica gel column. MAL conjugated TPE (TPE-MAL) was obtained as white powder. ^{1}H NMR (500 MHz, DMSO-d6) δ 2.08 (t, 2H), 2.56 (t, 2H), 3.09 (s,2H), 3.59 (s, 2H), 4.40 (s, 2H), 6.72 (d, 2H), 6.86 (d,2H), 6.96 (q, 6H), 7.11 (m, 9H). ^{13}C NMR (125 MHz, $CDCl_3$) δ 26.91, 34.25, 37.15, 51.49, 66.05, 113.91, 126.54, 127.74, 130.61, 131.80, 135.93, 139.81, 143.39, 154.08, 156.26, 172.46, 175.01. MS (EI): M+m/z 548.5.

Synthesis of Biotin-PEG-CHO: Biotin-PEG-CHO was synthesized as illustrated in Scheme S4 (Supporting Information). 400 mg of Biotin-PEG5000-NH_2 and 100 mg of succinimidyl 4-formylbenzoate were added into 15 mL of DMF. The mixture was stirred at room temperature for 72 h. The solution was then dialyzed against DMF and then water (MWCO 3500). After dialysis, the solution was lyophilized to obtain Biotin-PEG-CHO. The NMR results are presented in the Supporting Information with characteristic peaks labeled.

Synthesis of Biotin-PEG-MAL-TPE: Biotin-PEG-MAL-TPE was synthesized as illustrated in Scheme S4 (Supporting Information). 250 mg of Biotin-PEG5000-CHO and 274 mg of TPE-MAL were added into 10 mL of DMSO. The mixture was degassed three times using the freeze-pump-thaw procedure and reacted at 40 °C for 72 h. the solution was then dialyzed against DMSO and then water at pH 8.0 (MWCO 3500). After dialysis, the solution was lyophilized to obtain Biotin-PEG-MAL-TPE. The NMR results with characteristic peaks labeled and FT-IR analysis are presented in the Supporting Information.

Synthesis of Biotin-PEG-TPE: Biotin-PEG-TPE was synthesized as previously described and illustrated in Scheme S5 (Supporting Information).[43] 162 mg of TPE-COOH was dissolved in 10 mL of CH_2Cl_2. 82 mg of DCC and 49 mg of DMAP were then added. After stirring for 0.5 h, 200 mg of Biotin-PEG5000-NH_2 was added. The solution was stirred continuously at room temperature for 96 h. The solution was then dialyzed against DMSO and then distilled water (MWCO 3500). After dialysis, the solution was lyophilized to obtain Biotin-PEG-TPE. The NMR results with characteristic peaks labeled and FT-IR analysis are presented in the Supporting Information.

Synthesis of PEG-CHO: PEG-CHO was synthesized as illustrated in Scheme S6 (Supporting Information). 400 mg of PEG5000-NH_2 and 100 mg of succinimidyl 4-formylbenzoate were added into 15 mL of DMF. The mixture was stirred at room temperature for 72 h. The solution was then dialyzed against DMF and then water (MWCO 3500). After dialysis, the solution was lyophilized to obtain PEG-CHO. The NMR results are presented in the Supporting Information with characteristic peaks labeled.

Synthesis of PEG-MAL-TPE: PEG-MAL-TPE was synthesized similar to Biotin-PEG-MAL-TPE and illustrated in Scheme S6 (Supporting Information). 250 mg of mPEG5000-CHO and 274 mg of TPE-MAL were added into 10 mL of DMSO. The mixture was degassed three times using the freeze-pump-thaw procedure and reacted at 40 °C for 72 h. The solution was then dialyzed against DMSO and then water at pH 8.0 (MWCO 3500). After dialysis, the solution was lyophilized to obtain PEG-MAL-TPE. The NMR results with characteristic peaks labeled and FT-IR analysis are presented in the Supporting Information.

pH-Responsive Fluorescence Lightup of Biotin-PEG-MAL-TPE: Biotin-PEG-MAL-TPE was added into PBS (10×10^{-3} M, pH 5.0) with the final concentrations of 50×10^{-6} M. The mixed solution was incubated at 37 °C and the fluorescence spectra were recorded at designated time with the excitation wavelength of 360 nm.

Cell Culture: Human lung adenocarcinoma epithelial cells (A549 cells) were cultured in F-12K medium containing 10% fetal bovine serum (FBS) in 5% CO_2 at 37 °C. Human umbilical vein endothelial cells (HUVECs) were cultured in RPMI 1640 medium containing 10% FBS in 5% CO_2 at 37 °C.

Fluorescent Microscopy: A549 cells were seeded and incubated in 24 well plates (1×10^5 cells per well) in F-12K medium. After 24 h incubation, the medium was replaced with fresh serum-free medium. The bioprobe (Biotin-PEG-MAL-TPE, PEG-MAL-TPE, or Biotin-PEG-TPE) was added with the final concentration of 50×10^{-6} M. After incubation for 8 h, the medium was removed and the cells were washed by PBS for three times. The fluorescence images of A549 cells were observed by fluorescence microscope. For the cell uptake of Biotin-PEG-MAL-TPE bioprobe by HUVEC cells, HUVEC cells were seeded and incubated in 24 well plates (1×10^5 cells per well) in RPMI 1640 medium. After 24 h incubation, the medium was replaced with fresh serum-free medium. The Biotin-PEG-MAL-TPE bioprobe was added with the final concentration of 50×10^{-6} M. After incubation for 8 h, the medium was removed and the cells were washed by PBS for three times. The fluorescence images of HUVEC cells were observed by fluorescence microscope.

Endocytosis Mechanism Investigation: A549 cells were seeded in confocal dishes at 3×10^4 cells per well and incubated for 12 h at 37 °C. For the ATP-depletion studies, the cells were pretreated with 10×10^{-3} M NaN_3 and 50×10^{-3} M 2-deoxy-D-glucose for 30 min at 37 °C. Then, the medium was replaced with 10×10^{-6} M Biotin-PEG-MAL-TPE in fresh culture medium. For low temperature incubation at 4 °C, the medium was replaced with 10×10^{-6} M Biotin-PEG-MAL-TPE in fresh culture medium incubated at 4 °C, instead of the regular 37 °C condition. The medium replaced with 10×10^{-6} M Biotin-PEG-MAL-TPE in fresh culture medium without treatment was used as parallel group. After incubation with Biotin-PEG-MAL-TPE for 3 h, the medium was removed and the cells were washed with PBS for three times. The fluorescence images of Biotin-PEG-MAL-TPE in cells were observed by fluorescence microscope.

Cell Apoptosis: A549 cells were seeded in a 24-well plate (3×10^5 cells per well) and cultured for 24 h. The medium was replaced with fresh serum-free medium. Biotin-PEG-MAL-TPE or PEG-MAL-TPE was added with final concentration of 50×10^{-6} M. After incubation for 8 h, the samples were irradiated with a 635 nm laser at 500 mW cm^{-2} for 1 min. After incubation for 12 h, cells were treated with trypsin and centrifuged for 5 min at 1000 rpm after being washed with PBS for three times. The cells were then suspended in 500 µL binding buffer. 5 µL Annexin V-FITC and 5 µL PI were then added and incubated with the cells for 15 min in the dark. Finally, the stained cells were analyzed using a FACScan flow cytometer.

Reactive Oxygen Generation Measurement: A549 cells were seeded and incubated in 96-well plates (1×10^4 cells per well) with F-12K medium for 24 h. The prodrug Biotin-PEG-MAL-TPE or PEG-MAL-TPE was then added with final concentration of 50×10^{-6} M. After incubation for 8 h, the medium was replaced by 40 µL serum

DOI: 10.1002/smll.201600950

free medium containing 10×10^{-6} M DCFDA. After incubation for another 0.5 h, the cells were washed with serum free medium. After irradiated with a 635 nm laser at 500 mW cm^{-2} for 0.5 min and washed with serum free medium, the fluorescence images were observed using a fluorescence microscope.

Cytotoxicity Assay: A549 cells were seeded and incubated in 96-well plates (1×10^4 cells per well) with F-12K medium for 24 h. The prodrug Biotin-PEG-MAL-TPE, PEG-MAL-TPE, or free MAL was added in different concentrations ($5–50 \times 10^{-6}$ M). After incubation for 8 h, the samples were irradiated by a 635 nm laser at 500 mW cm^{-2} for 5 min. The cells were then cultured for another 12 h. For MTT test, 20 µL MTT (5 mg mL^{-1}) per well was added and the cells were incubated for another 4 h. Then the culture media in each well was replaced by 150 µL DMSO. The absorbance was measured at a wavelength of 490 nm. Data were expressed as average ± SD ($n = 4$). In order to measure the dark cytotoxicity of Biotin-PEG-MAL-TPE prodrugs, PEG-MAL-TPE prodrugs, and free MAL against A549 cells, A549 cells with light irradiation were adopted. Meanwhile, different influence factors, such as light irradiation time, and light intensity were studied to evaluate the photodynamic cytotoxicity of Biotin-PEG-MAL-TPE prodrugs, PEG-MAL-TPE prodrugs, and free MAL using the same method.

Supporting Information

Supporting Information is available from the Wiley Online Library or from the author.

Acknowledgements

Financial support from the National Natural Science Foundation of China (Grant Nos. 51303154, 51573160, and 21574114), the Key Science Technology Innovation Team of Zhejiang Province (Grant No. 2013TD02), and the Fundamental Research Funds for the Central Universities (Grant No. 2016QNA4033) is gratefully acknowledged.

[1] R. Kumar, W. S. Shin, K. Sunwoo, W. Y. Kim, S. Koo, S. Bhuniya, J. S. Kim, *Chem. Soc. Rev.* **2015**, *44*, 6670.
[2] Y. Guo, W. J. Chen, W. W. Wang, J. Shen, R. M. Guo, F. M. Gong, S. D. Lin, D. Cheng, G. H. Chen, X. T. Shuai, *ACS Nano* **2012**, *6*, 10646.
[3] N. Ahmed, H. Fessi, A. Elaissari, *Drug Discovery Today* **2012**, *17*, 928.
[4] S. Capece, E. Chiessi, R. Cavalli, P. Giustetto, D. Grishenkove, G. Paradossi, *Chem. Commun.* **2013**, *49*, 5763.
[5] T. D. Ashton, K. A. Jolliffe, F. M. Pfeffe, *Chem. Soc. Rev.* **2015**, *44*, 4547.
[6] J. Liang, B. Z. Tang, B. Liu, *Chem. Soc. Rev.* **2015**, *44*, 2798.
[7] Y. Hong, J. W. Y. Lama, B. Z. Tang, *Chem. Soc. Rev.* **2011**, *40*, 5361.
[8] J. Mei, J. Wang, J. Z. Sun, H. Zhao, W. Z. Yuan, C. Deng, S. Chen, H. H. Sung, P. Lu, A. Qin, H. S. Kwok, Y. Ma, I. D Williams, B. Z. Tang, *Chem. Sci.* **2012**, *3*, 549.
[9] A. Qin, J. W. Y. Lam, B. Z. Tang, *Prog. Polym. Sci.* **2012**, *37*, 182.
[10] D. Ding, K. Li, B. Liu, B. Z. Tang, *Acc. Chem. Res.* **2013**, *46*, 2441.
[11] Y. Yuan, C. J. Zhang, M. Gao, R. Zhang, B. Z. Tang, B. Liu, *Angew. Chem. Int. Ed.* **2015**, *54*, 1780.
[12] H. J. Han, Q. Jin, Y. Wang, Y. J. Chen, J. Ji, *Chem. Commun.* **2015**, *51*, 17435.
[13] Y. Yuan, R. T. Kwok, B. Z. Tang, B. Liu, *J. Am. Chem. Soc.* **2014**, *136*, 2546.
[14] X. Xue, Y. Zhao, L. Dai, X. Zhang, X. Hao, C. Zhang, S. Huo, J. Liu, C. Liu, A. Kumar, W. Q. Chen, G. Zou, X. J. Liang, *Adv. Mater.* **2014**, *26*, 712.
[15] K. Dhara, Y. Hori, R. Baba, K. Kikuchi, *Chem. Commun.* **2012**, *48*, 11534.
[16] S. Li, S. M. Langenegger, R. Haner, *Chem. Commun.* **2013**, *49*, 5835.
[17] Y. Yuan, R. T. K. Kwok, G. Feng, J. Liang, J. Geng, B. Z. Tang, B. Liu, *Chem. Commun.* **2014**, *50*, 295.
[18] A. P. Castano, M. Pawel, M. R. Hamblin, *Nat. Rev. Cancer* **2006**, *6*, 535.
[19] K. Han, S. B. Wang, Q. Lei, J. Y. Zhu, X. Z. Zhang, *ACS Nano* **2015**, *9*, 10268.
[20] S. S. Lucky, K. C. Soo, Y. Zhang, *Chem. Rev.* **2015**, *115*, 1990.
[21] K. Han, Q. Lei, S. B. Wang, J. J. Hu, W. X. Qiu, J. Y. Zhu, W. N. Yin, X. Luo, X. Z. Zhang, *Adv. Funct. Mater.* **2015**, *25*, 2961.
[22] T. Wang, N. Zabarska, Y. Z. Wu, M. Lamla, S. Fischer, K. Monczak, D. Y. W. Ng, S. Rau, T. Weil, *Chem. Commun.* **2015**, *51*, 12552.
[23] N. L. Oleinick, R. L. Morris, I. Belichenko, *Photochem. Photobiol. Sci.* **2002**, *1*, 1.
[24] Q. Peng, K. Berg, J. Moan, M. Kongshaug, J. M. Nesland, *Photochem. Photobiol.* **1997**, *65*, 235.
[25] M. Wachowska, A. Muchowicz, M. Firczuk, M. Gabrysiak, M. Winiarska, M. Wańczyk, K. Bojarczuk, J. Golab, *Molecules* **2011**, *16*, 4140.
[26] X. Ma, Q. Qu, Y. Zhao, *ACS Appl. Mater. Interfaces* **2015**, *7*, 10671.
[27] C. W. Chung, K. D. Chung, Y. I. Jeong, D. H. Kang, *Int. J. Nanomed.* **2013**, *8*, 809.
[28] M. Benito, V. Martin, M. D. Blanco, J. M. Teijon, C. Gomez, *J. Pharm. Sci.* **2013**, *102*, 2760.
[29] R. P. Johnson, C. W. Chung, Y. I. Jeong, D. H. Kang, H. Suh, I. Kim, *Int. J. Nanomed.* **2012**, *7*, 2497.
[30] D. L. Ni, J. W. Zhang, W. B. Bu, H. Y. Xing, F. Han, Q. F. Xiao, Z. W. Yao, F. Chen, Q. J. He, J. N. Liu, S. J. Zhang, W. P. Fan, L. P. Zhou, W. J. Peng, J. L. Shi, *ACS Nano* **2014**, *8*, 1231.
[31] Q. Peng, T. Warloe, K. Berg, J. Moan, M. Kongshaug, K. E. Giercksky, J. M. Nesland, *Cancer* **1997**, *79*, 2282.
[32] H. X. Tong, Y. Wang, H. Li, Q. Jin, J. Ji, *Chem. Commun.* **2016**, *52*, 3966.
[33] V. Delplace, P. Couvreur, J. Nicolas, *Polym. Chem.* **2014**, *5*, 1529.
[34] Y. Xin, J. Y. Yuan, *Polym. Chem.* **2012**, *3*, 3045.
[35] S. C. Silverstein, R. M. Steinman, Z. A. Cohn, *Annu. Rev. Biochem.* **1977**, *46*, 669.
[36] N. Wong, S. Kam, Z. Liu, H. Dai, *Angew. Chem. Int. Ed.* **2006**, *45*, 577.
[37] S. Bhuniya, S. Maiti, E. J. Kim, H. Lee, J. L. Sessler, K. S. Hong, J. S. Kim, *Angew. Chem. Int. Ed.* **2014**, *53*, 4469.
[38] W. H. Chen, G. F. Luo, Q. Lei, H. Z. Jia, S. Hong, Q. R. Wang, R. X. Zhuo, X. Z. Zhang, *Chem. Commun.* **2015**, *51*, 465.
[39] D. L. Ni, J. W. Zhang, W. B. Bu, H. Y. Xing, F. Han, Q. F. Xiao, Z. W. Yao, F. Chen, Q. J. He, J. A. Liu, S. J. Zhang, W. P. Fan, L. P. Zhou, W. J. Peng, J. L. Shi, *ACS Nano* **2014**, *8*, 1231.
[40] H. B. Wang, G. Y. Liu, H. Gao, Y. B. Wang, *Polym. Chem.* **2015**, *6*, 4715.
[41] J. A. Phillips, E. L. Morgan, Y. Dong, G. T. Cole, C. McMahan, C. Y. Hung, S. D. Sanderson, *Bioconjugate Chem.* **2009**, *20*, 1950.
[42] H. B. Wang, Y. Huang, X. Zhao, W. Gong, Y. Wang, Y. Y. Cheng, *Chem. Commun.* **2014**, *50*, 15075.
[43] C. Q. Zhang, S. B. Jin, S. L. Li, X. D. Xue, J. Liu, Y. R Huang, Y. G. Jiang, W. Q. Chen, G. Z. Zou, X. J. Liang, *ACS Appl. Mater. Interfaces* **2014**, *6*, 5212.

Received: March 19, 2016
Revised: May 8, 2016
Published online: